Available online at www.sciencedirect.com

ScienceDirect

www.elsevier.com/locate/jes

JES JOURNAL OF ENVIRONMENTAL SCIENCES

www.jesc.ac.cn

A nanofilter composed of carbon nanotube-silver composites for virus removal and antibacterial activity improvement

Jun Pyo Kim, Jae Ha Kim, Jieun Kim, Soo No Lee, Han-Oh Park*

Nano Development Team, Bioneer Corporation, Daejeon 306-220, Republic of Korea. E-mail: nanobiojpk@bioneer.co.kr

ARTICLE INFO

Article history:
Received 26 June 2014
Revised 6 November 2014
Accepted 11 November 2014
Available online 1 December 2015

Keywords:
Carbon nanotube
Silver nanoparticle
Virus removal
Nanofilter
Water purification

ABSTRACT

We have developed a new nanofilter using a carbon nanotube-silver composite material that is capable of efficiently removing waterborne viruses and bacteria. The nanofilter was subjected to plasma surface treatment to enhance its flow rate, which was improved by approximately 62%. Nanoscale pores were obtained by fabricating a carbon nanotube network and using nanoparticle fixation technology for the removal of viruses. The pore size of the nanofilter was approximately 38 nm and the measured flow rate ranged from 21.0 to 97.2 L/(min·m^2) under a pressure of 1–6 kgf/cm^2 when the amount of loaded carbon nanotube-silver composite was 1.0 mg/cm^2. The nanofilter was tested against Polio-, Noro-, and Coxsackie viruses using a sensitive real-time polymerase chain reaction assay to detect the presence of viral particles within the outflow. No trace of viruses was found to flow through the nanofilter with carbon nanotube-silver composite loaded above 0.8 mg/cm^2. Moreover, the surface of the filter has antibacterial properties to prevent bacterial clogging due to the presence of 20-nm silver nanoparticles, which were synthesized on the carbon nanotube surface.

Introduction

The continued advancements in the field have shown that filter separation of particles from fluids to achieve high purity is a critical area in research and development of industrial technologies. Nanoparticle separation is becoming increasingly important as needs arise in diverse fields including the semiconductor, chemical, food, pharmaceutical, medical, and biochemical industries, as well as the environmental field. Especially in the environmental field, where the need for clean water and awareness of water shortages has increased, nanofiltration technology is a potentially viable solution.

Since their discovery in 1991 (Iijima, 1991), carbon nanotubes (CNTs) have attracted much attention in various scientific communities, with a myriad of applications in electronics, composite materials, fuel cells, sensors, optical devices, and biomedicine. Moreover, CNTs, because of their high surface area, electronic properties, and ease of functionalization, have excellent nanosorbent properties for filtering contaminants from water (Diallo and Savage, 2005; Upadhyayula et al., 2009). Previous studies in this field have focused on the use of bare CNTs or CNTs functionalized with inorganic nanoparticles for adsorption of inorganic contaminants and toxic metals from water (Di et al., 2006; Li et al., 2003; Peng et al., 2005). Other studies have explored the use of CNTs for adsorption of low molecular weight organic contaminants (Lu et al., 2005) and toxins (Yan et al., 2006) from water.

In particular, CNTs have been studied as filters for the removal of viruses or bacteria. Single-walled carbon nanotube

* *Corresponding author.*

http://dx.doi.org/10.1016/j.jes.2014.11.017

(SWCNT) filters have shown high bacterial retention (Brady-Estévez et al., 2008), and multi-walled carbon nanotube (MWCNT) filters have high viral removal efficiency at low pressure (Brady-Estévez et al., 2010a), both through the effects of size exclusion. Moreover, a SWCNT-MWCNT hybrid filter achieved efficient bacterial inactivation and viral retention at low pressure (Brady-Estévez et al., 2010b). The application of an external electric field markedly enhanced the viral removal by the CNT filter, because of the increased viral particle transport (Rahaman et al., 2012). Furthermore, in order to enhance the antibacterial ability of the CNT filter, vertically aligned MWCNT arrays were combined with silver nanoparticles (Akhavan et al., 2011), and CNT/cotton membrane was combined with silver nanowires (Schoen et al., 2010). A recent study demonstrated scalable applications of this technology that use low-cost and widely available CNTs for inactivation of microbes (Kang et al., 2008a,b, 2009). For viral removal by CNT-hybrid filters, filtration performance was also tested under various solution chemistries (Brady-Estévez et al., 2010c). These CNT-based filters remove the micrometer-sized bacterial cells through a sieving mechanism, whereas depth (physicochemical) filtration governs the adsorption of nano-scale viruses throughout the thickness of the matrix.

In this study, we describe a novel, highly permeable, MWCNT-silver (Ag) nanofilter and demonstrate its use for the effective removal of bacterial and viral pathogens from water at low pressure. Although previous studies have provided a proof-of-concept for viral removal by filters of various forms using CNTs, a CNT-Ag nanofilter in which Ag nanoparticles are synthesized on the CNT surface has not been reported. This filter was fabricated by utilizing the following key properties of CNTs and Ag nanoparticles: (1) the small diameter and high surface area of CNTs; (2) the tendency of CNTs to aggregate and form highly porous structures; (3) the low melting point of Ag nanoparticles; and (4) the antibacterial activity of Ag nanoparticles. We demonstrated that bacteria were completely retained on the CNT-Ag nanofilter and were effectively inactivated upon contact with Ag on the MWCNT. We also showed that viruses could be completely removed by a depth-filtration mechanism, that is, capture by nanotube bundles inside the CNT-Ag layer.

1. Materials and methods

1.1. Materials

MWCNTs were provided by Hanwah Nanotech (CM-95 grade) in South Korea. Polyvinylpyrrolidone (PVP) was purchased from Fluka (Mw: 40,000). Ethylene glycol, sodium dodecyl sulfate (SDS), oleylamine, silver nitrate ($AgNO_3$), ethyl acetate, and hexane were purchased from Sigma-Aldrich. Poliovirus 1 (ATCC No. VR-1562), Coxsackie type A9 virus (coxA9 virus, ATCC No. VR-186), and Norovirus GI RNA (ATCC No. VR-3199) were purchased from the American Tissue Culture Collection (ATCC). *Staphylococcus aureus* (KCTC 1928) and *Escherichia coli* (KCTC 1039) were purchased from the Korean Collection for Type Culture (KCTC).

1.2. Preparation of the CNT-Ag composite

Thin MWCNTs (0.3 g) were loaded into a 500-mL round flask reactor, to which 280 mL of ethylene glycol was added, followed by stirring for 30 min. Ethylene glycol acts as a weak reductant that slows down the growth of the Ag nuclei. (Ducamp-Sanguesa et al., 1993). Subsequently, the reactor was placed in an ultrasonic cleaner, followed by dispersion of the carbon nanotubes in ethylene glycol for 3 hr using ultrasonic waves at a temperature of under 50°C. Post-ultrasonication, a stirrer was attached to the reactor and a thermometer and condenser, for cooling, were connected. While stirring the reactor, 1.68 g of PVP and 5.6 mL of oleylamine, to which 1.102 g of $AgNO_3$ was added in a stepwise manner, were added. A vacuum pump was connected to replace air in the reactor with nitrogen. While the nitrogen was continuously supplied, nitrogen was forced to circulate within the reactor to prevent oxygen inflow. A mantle was attached to the bottom of the flask and the temperature of the reactor was raised to 200°C for 40 min, followed by reduction for 1 hr. The temperature of the reactor was lowered slowly to room temperature for 3 hr upon completion of reduction. The generated CNT-Ag composites were filtered with a filter paper, followed by washing with ethyl acetate and hexane several times (Cha et al., 2005; Kim et al., 2007, 2008).

1.3. CNT-Ag nanofilter preparation

The generated CNT-Ag was uniformly coated on a glass fiber (GF) membrane with a pore size of 0.7 μm (Whatman, USA) by using a sonication/filtration procedure. Specified quantities of CNT-Ag (0.03–0.15 g) were suspended in 500 mL of deionized water containing 0.5 g of SDS. The suspension was sonicated for 1 hr, and then vacuum-filtered through a GF membrane to achieve the various loadings of CNT-Ag on the base filters. Ethanol (100 mL) followed by 500 mL of deionized water were passed through the CNT-Ag nanofilter to remove residual SDS and ethanol. Then, the fabricated CNT-Ag nanofilter was dried in an oven for 12 hr at 60°C. Finally, the CNT-Ag nanofilter was heat-treated for 10 min at 250°C.

1.4. Characterization of CNT-Ag composite and nanofilter

A field-emission transmission electron microscope (FE-TEM, JEOL, JEM-2010, Japan) at an acceleration voltage of 200 kV was used to investigate the size and distribution of the silver on the CNT surface. TEM specimens were prepared by placing a few drops of sample solutions on a carbon grid. The crystalline structures of the synthesized CNT-Ag nanocomposite were investigated using an X-ray diffractometer (XRD). Lyophilized and powdered samples were used, and the diffraction patterns were recorded in the scanning mode on an X'pert Pro diffractometer (PANalytical, Almelo, the Netherlands) operated at 40 kV and with a current of 30 mA, with Cu/$k\alpha$ radiation (λ = 1.5418 Å) in the range of 20°–80° 2θ.

The surface morphology of the CNT-Ag nanofilter was studied using field emission scanning electron microscopy (FE-SEM, S-4300SE, Hitachi, Japan). Wettability measurements were performed using a Video-Based Optical Contact Angle Meter (Dataphysics, OCA15EC). Distilled water was used as the

liquid for the static water contact angle measurement. The surface chemical compositions of plasma-treated and untreated CNT-Ag filters were analyzed using an X-ray photoelectron spectroscopy system (XPS, Thermo ESCALAB 250) equipped with a Mg Kα X-ray source with pass energy of 1253.6 eV. The analysis was carried out under 10^{-9}–10^{-10} Torr with power of 300 W. Photo-emitted electrons were collected at a take-off angle of 45° and the deconvolution analysis of C1s peaks was carried out using XPS Peak software. To analyze the pore size, CNT-Ag–coated glass filters (CNT loading amounts: 0.8, 1.0 mg/cm^2) were tested. The pore size of the CNT-Ag coated on the glass filter was analyzed using a capillary flow porometer after drying at 75°C for 24 hr. Pore size analysis was performed by a third party at Korea Institute of Industrial Technology and the test conditions are shown in Table 1. The filtration system consisted of a 47-mm diameter stainless steel holder (Bioneer Corp.) to support the membranes and a pressurized tank system. The flow rate of the prepared CNT-Ag nanofilters was evaluated by measurement of water volume per minute through the filter holder at different pressures. Differential thermal analysis (DTA) was performed for the heat analysis of Ag nanoparticles in a TA instrument (SDT 2960) with a heating rate of 10°C/min from 50°C to 250°C in a nitrogen atmosphere with a gas flux of 200 mL/min.

1.5. Plasma treatment

To modify the surface of the CNT-Ag nanofilter, atmospheric-pressure plasma surface treatment was employed using an ATMOS Multi boiler (PLASMART Ltd., South Korea). The gas used in the plasma treatment was Ar (99.999% purity), which was introduced into the chamber at a flow rate of 5 L/min. The plasma treatment power was maintained at 100 W at a frequency of 13.56 MHz. The fabricated CNT-Ag nanofilter sample was moved on a translation stage through the plasma jet at a speed of 0.5 cm/sec for a single treatment. The plasma treatment was performed five times for 2 min at room temperature and atmospheric pressure (Liu et al., 2013).

1.6. Filtration and antibacterial activity test

The CNT-Ag nanofilters were tested for their ability to remove various viruses and bacteria from water. For inactivation, the coxA9 virus, Norovirus, and Poliovirus (each at a load of 1.1×10^4 copies/mL) were suspended in 10 mL of deionized water and heat-treated at 100°C for 20 min. Inactive viruses were filtered through the CNT-Ag nanofilter and the GF membrane (pore size = 0.7 μm; control). Filter efficiency was calculated by counting the difference between the amount of contaminant concentration in the water before and after the filtration. To evaluate bacteria removal, *S. aureus* and *E. coli* were grown in brain heart infusion (BHI) liquid medium at 37°C and harvested at mid-exponential growth phase. Cells were rinsed and centrifuged twice (2000 rpm, 10 min), and then diluted to a concentration of the 103 CFU/mL. After filtration with the CNT-Ag nanofilter, cells were cultivated on a BHI agar plate for 24 hr at 37°C. To study the antibacterial activity of the CNT-Ag nanofilter, *S. aureus* and *E. coli* cells (103 CFU/mL) were smeared on a BHI agar plate containing the CNT-Ag nanofilter. Then, the cells were incubated for 24 hr at 37°C.

Table 1 – Test conditions for pore size measurement.

	Test condition
Testing M/C	Automated capillary flow porometer
Model	CFP-1200AEL
Producing company	Porous Materials Inc.
Test method	ASTM F 316
Sample diameter	2.1 cm
Test type	Dry up/wet up
Fluid	Porewick (surface tension: 16.0 dyn/cm)
Test Pressure	0–160 psi

1.7. Virus quantification by real-time quantitative polymerase chain reaction

Extraction of virus ribonucleic acid (RNA) was performed using the Exiprep™ 16 Plus (Cat. No. A-5030, Bioneer Corp., South Korea) instrument and the Exiprep™ Viral RNA Extraction kit (Cat No. K-3535, Bioneer Corp., South Korea). The master mix was prepared as follows: 45 μL of master mix was added to AccuPower®Enterovirus Real-Time reverse-transcription quantitative polymerase chain reaction (Real-Time RT-qPCR) kit wells (Cat No. ENT-1111, Bioneer Corp., South Korea), and then 5 μL of extracted viral RNA was added to the wells of the AccuPower®Enterovirus Real-Time RT-qPCR kit. A one-step real-time RT-qPCR assay was performed using the Exicycler™ 96 (Cat No. A-2060, Bioneer Corp., South Korea). The qPCR mixture was incubated 15 min at 45°C for complementary deoxyribonucleic acid (cDNA) synthesis, followed by 5 min at 95°C to activate DNA polymerase. Subsequently, 45 cycles consisting of a denaturation step for 5 sec at 95°C and combined annealing-extension step for 20 sec at 55°C were performed. After the annealing-extension step, the amplification was monitored by quantitatively analyzing fluorescence emission. The probe for the internal positive control (IPC) was the carboxytetramethylrhodamine dye, and all the wells were set with the appropriate probes. The samples were placed in the Exicycler™ 96 as indicated in the manufacturer's instructions. After the reaction was complete, the accompanying Exicycler™ 96 analysis program was used to analyze the results.

2. Results and discussion

2.1. Structural characterization of CNT-Ag powder

CNT-Ag composite powders were fabricated by a proprietary 'polyol process' as mentioned in Section 1.2. A "polyol process" for the synthesis of metal nanoparticles been previously reported by many research groups (Ayyappan et al., 1996; Hinotsu et al., 2004; Cha et al., 2005; Kim et al., 2007, 2008). It basically involves the chemical reduction of a metallic compound by a liquid polyol, which also acts as solvent and dispersing agent, nucleation of metal atoms, and growth of the metallic nuclei. Fig. 1a shows FE-TEM images of the CNT-Ag composite synthesized by our polyol process. Ag nanoparticles with average diameters of about 20 nm are distributed on CNTs

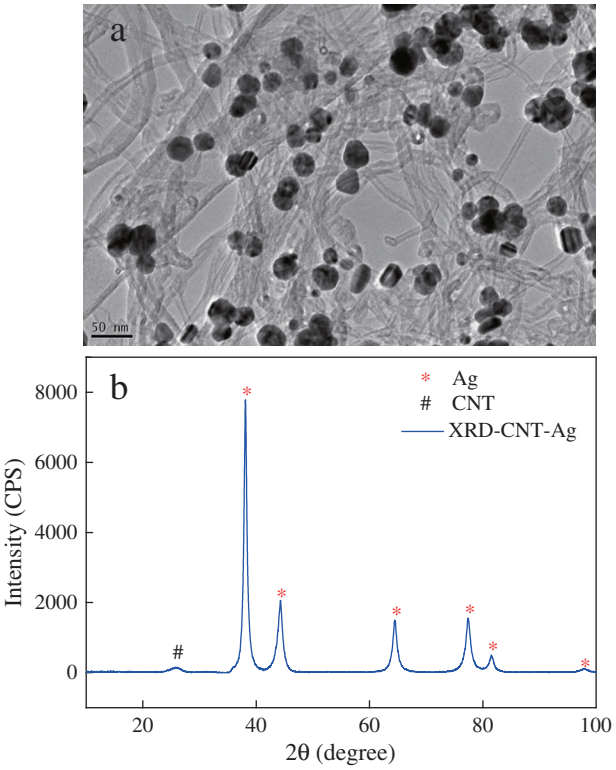

Fig. 1 – Characterization of CNT-Ag nanocomposites. (a) FE-TEM image of CNT-Ag. (b) XRD pattern of CNT-Ag nanocomposites. CNT: carbon nanotube; FE-TEM: field-emission transmission electron microscope; XRD: X-ray diffractometer.

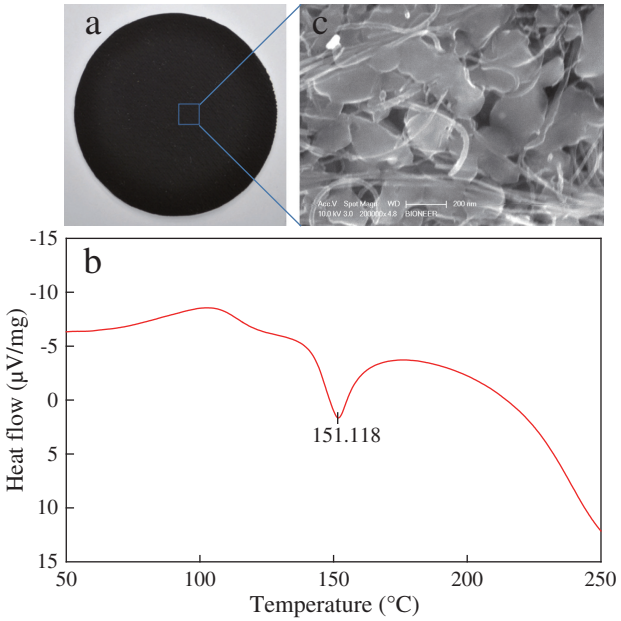

Fig. 2 – Structure of the nanofilter made from the CNT-Ag powder. (a) Image of CNT-Ag-coated glass filter (Ö47 mm). (b) DTA curves of the CNT-Ag composite at a heating rate of 10°C/min. (c) SEM image of the CNT-Ag composite material after heat treatment at 250°C for 10 min. CNT: carbon nanotube; SEM: scanning electron microscopy.

with diameters of 10–40 nm. The CNT-Ag nanocomposites were analyzed by XRD as shown in Fig. 1b. The XRD pattern of the CNT-Ag nanocomposites showed peaks at 26°, 38°, 44°, 64°, 77°, and 81°. The diffraction peaks at 2θ of 38°, 44°, 64°, 77°, and 81° were readily indexed to (111), (200), (220), (311), and (222) reflections of silver metal crystals on both hybrid structures, respectively, representing the face-centered cubic (fcc) phase of silver. The peak at 26° with prominent peak counts showed the presence of CNTs, being readily indexed to the (002) reflection of CNTs (Park and Gong, 2012; Kim et al., 2012).

2.2. Structural characterization of the nanofilter made from CNT-Ag powder

The filter was developed using a GF-based microporous membrane (pore size = 0.7 μm) uniformly covered with a thin layer of CNT-Ag. Fig. 2a presents a CNT-Ag nanofilter fabricated by deposition of 0.8-mg/cm^2 CNT-Ag composites onto the Ö47 GF membrane base of the filter. As illustrated in Fig. 2b, the DTA heating curve for the CNT-Ag composite is shown. A change of the heat flow was observed at 151.1°C, which corresponds to the melting temperature (T_m) of the Ag nanoparticles. Since the size of the metal was in the nanoscale, its melting point was at approximately 150°C. Accordingly, when heat treatment was performed at relatively low temperatures, the silver nanoparticles melted and generated a carbon nanostructure-silver metal composite with a network structure. The carbon nanostructure-silver metal composite and the membrane support were well combined (Fig. 2c).

2.3. Flow rate of the CNT-Ag nanofilter

To measure the flow rate of the CNT-Ag nanofilter, 0.8 mg/cm^2 CNT-Ag powder was coated on a bare GF filter. The flow rate of

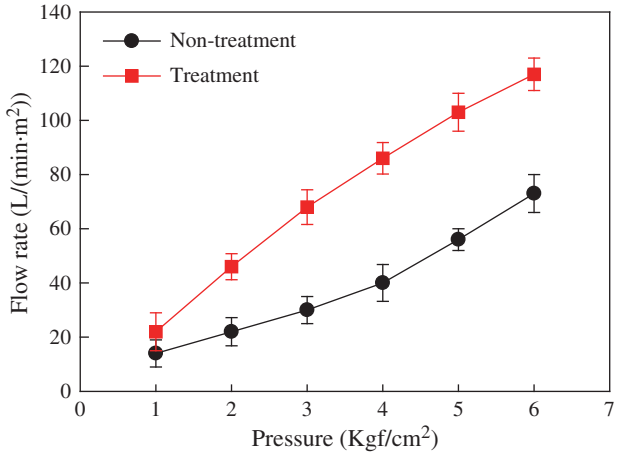

Fig. 3 – Comparison of the flow rate through the CNT-Ag nanofilter with and without surface plasma treatment. This experiment was repeated in each condition by three times. CNT: carbon nanotube.

the fabricated CNT-Ag nanofilter was measured at pressures varying from 1 to 6 kgf/cm^2 after it was mounted on the Ö47-mm stainless steel holder of the filtration system. As shown in Fig. 3, the flow rate of the fabricated CNT-Ag nanofilter increased depending on the pressure. However, the flow rate of an untreated CNT-filter was very low (72.4 L/(min·m^2)) even at high pressure (6 kgf/cm^2) because the pore size of the fabricated CNT-Ag nanofilter was in the nanoscale and the carbon nanotubes had highly hydrophobic surfaces (Liu et al., 2013). Thus, the flow of hydrophilic liquids such as water through the filter is hindered. Although CNTs are hydrophobic in nature, they can be made hydrophilic *via* plasma treatment.

Fig. 4 shows contact angle measurements for the CNT-Ag filter surface (a) before and (b) after plasma treatment. In order to determine to what extent the plasma treatment transformed hydrophobic surfaces to hydrophilic surfaces for the CNT-Ag filter, water contact angle tests were performed and the results are shown in Fig. 4. Water contact angles decreased from 131.6° for the control to 38.4° for the plasma-treated sample. This demonstrates clear evidence of wettability change, which is due to the presence of more hydrophilic groups induced by the plasma treatment. Fig. 5 shows changes in the stability of the CNT-Ag filter surface depending on time after plasma treatment. As shown, the CNT-Ag filter surface is very stable and maintains a constant hydrophilic surface for 7 days after plasma treatment.

To provide evidence of the presence of functional groups after plasma treatment, the CNT-Ag filter surface was analyzed by XPS. XPS analysis was conducted to identify the surface chemical composition changes of the CNT-Ag filter surface after plasma functionalization. The C1s spectra were deconvoluted into two characteristic Gaussian peaks (Fig. 6a), including C–C (284.6 ± 0.2 eV, 65.75%), and C–O (285.8 ± 0.2 eV, 23.14%) before plasma treatment. By contrast, Fig. 6b shows that the C1s spectra were deconvoluted into three characteristic Gaussian peaks, including C–C (284.6 ± 0.2 eV, 40.41%), C–O–C (285.15 ± 0.2 eV, 40.86%), and COOH; O–C═O (288.0 ± 0.2 eV, 4.94%) after plasma treatment. The C–O–C, COOH and O–C═O groups observed on the CNT-Ag filter surface likely resulted from plasma-induced oxidation. C–C and C–O ratios decreased after plasma treatment, while C–O–C, COOH and O–C═O increased.

To transform the hydrophobic CNT-Ag nanofilter into a hydrophilic surface, the CNT-Ag nanofilter was plasma treated as described in Section 1.5. After plasma treatment, the flow rate of the CNT-Ag nanofilter was increased up to 116 L/(min·m^2) at a pressure of 6 kgf/cm^2, which represented an improvement of approximately 62% over the untreated CNT-Ag nanofilter. Utilizing plasma treatment methods to modify the surface of CNT can improve the wettability of the CNT-Ag nanofilter (Liu et al., 2013; Wang et al., 2013; Zhao et al., 2012). The plasma treatment is an efficient approach to improve the flow rate of the CNT-Ag nanofilter due to the oxygen functionalization of the CNT surface. Therefore, our CNT-Ag nanofilters were finally treated with plasma.

To fabricate a CNT-Ag nanofilter for virus removal, CNT-Ag powder at various concentrations (0, 0.2, 0.4, 0.6, 0.8, and 1.0 mg/cm^2) was coated on a bare GF filter. The water-filtrate flux of the fabricated CNT-Ag nanofilter was measured at different pressures. Fig. 7 shows the water flow rate of various CNT loading amounts. In all cases, the flow rates gradually increased with pressure. The control filter (*i.e.*, GF filter without CNT-Ag coating) presented a maximum flow rate of 188.4 L/(min·m^2) at 6 kgf/cm^2. The flow rate of the control at all pressure points was higher than that of the CNT-Ag-coated GF filter, probably because of its larger pore size (0.7 μm). In

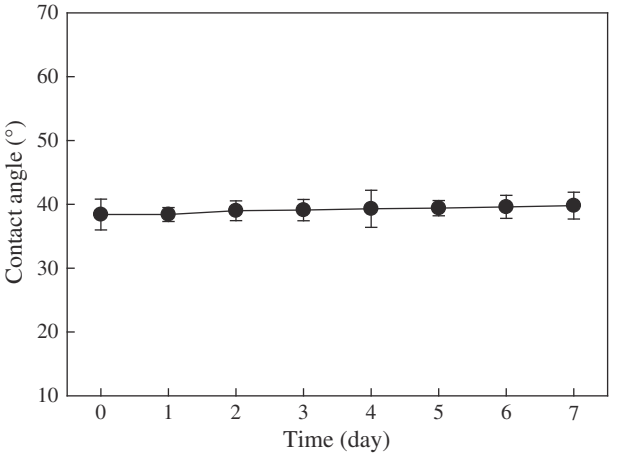

Fig. 5 – The stability of the functional groups on CNT-Ag filter surface after plasma treatment. This experiment was repeated in each condition by three times. CNT: carbon nanotube.

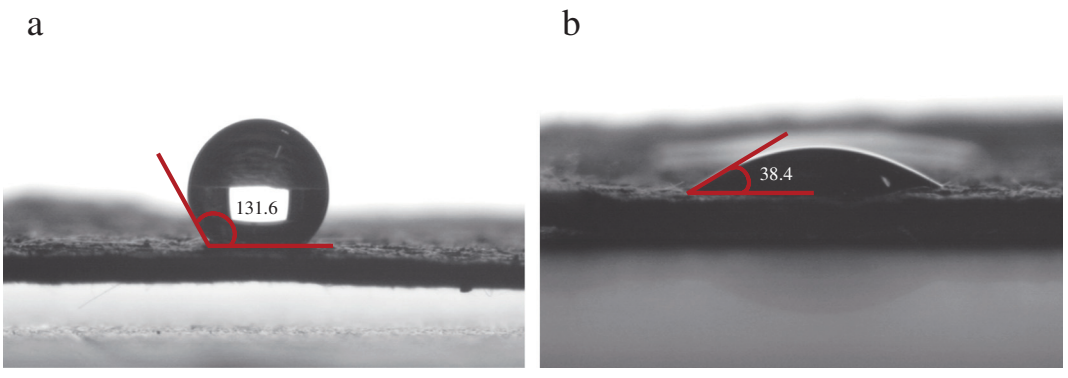

Fig. 4 – Contact angle measurement in CNT-Ag filter surface (a) before and (b) after plasma treatment. CNT: carbon nanotube.

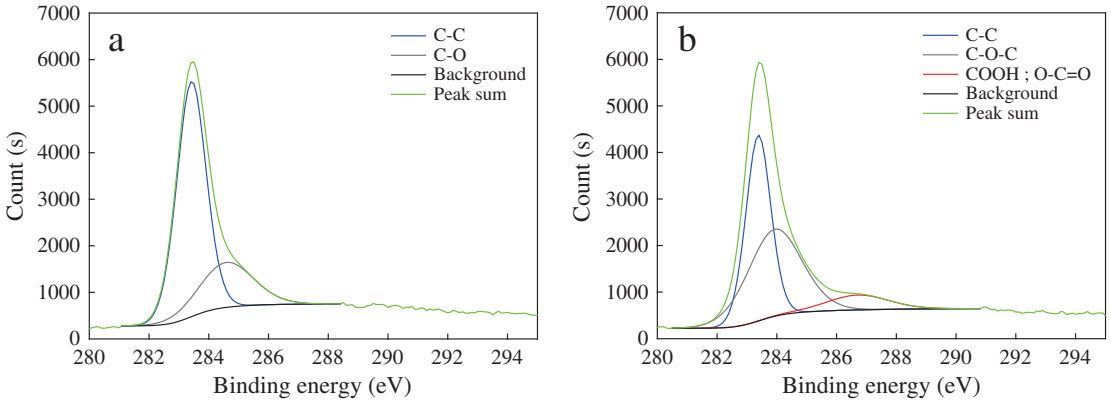

Fig. 6 – XPS C1s spectrum of (a) untreated and (b) plasma-treated on CNT-Ag filter surface. CNT: carbon nanotube; XPS: X-ray photoelectron spectroscopy.

contrast, the GF filter with 1.0 mg/cm^2 CNT-Ag coated on the surface, which had the smallest pore size, showed a low flow rate of 97.2 L/(min·m^2) at 6 kgf/cm^2. The flow rate of the CNT-Ag nanofilters decreased with increasing CNT-Ag coating amount. These results indicated that the pore size of the CNT-Ag nanofilter became smaller with higher CNT-Ag coating amounts.

2.4. *Virus-removal ability of the CNT-Ag nanofilter*

The fabricated CNT-Ag nanofilter was tested for its ability to remove waterborne viruses. CoxA9virus, which belongs to a family of non-enveloped, linear, single-stranded, and positive-sense ssRNA viruses *Picornaviridae* and the genus *Enterovirus*, was selected as the model virus. Enteroviruses are among the most common and important human pathogens and its members are normally transmitted through the fecal-oral route. The coxA9virus is approximately 30 nm in diameter and has icosahedral symmetry (Melnick et al., 1951). For the virus filtration experiments, equal concentrations of virus were filtered through the CNT-Ag-coated module (0.2, 0.4, 0.6, 0.8, and 1.0 mg/cm^2) and a bare GF filter as the control.

Fig. 8 presents the dependence of the residual virus concentration at the filter outlet (N/N$_0$) on the CNT-Ag layer thickness. Virus removal efficiency improved with the increase of CNT-Ag loading amount. At a CNT-Ag load of 0.8 mg/cm^2, viruses were completely removed in water. Fig. 9 shows the results of the real-time RT-qPCR analysis. The filtration test was performed with a 0.8 mg/cm^2-CNT-Ag nanofilter. As shown in Fig. 9a, coxA9 viruses were not

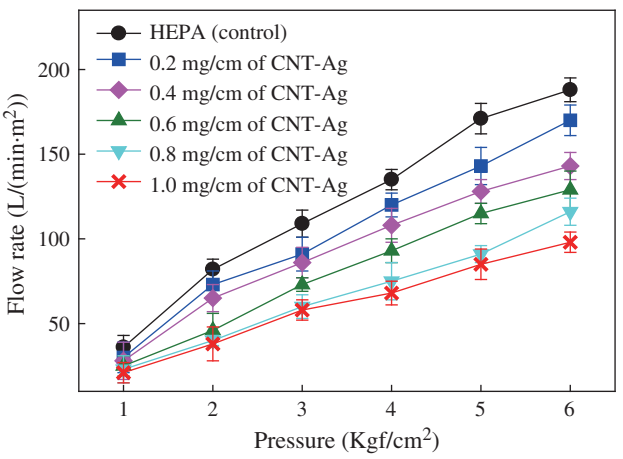

Fig. 7 – Comparison of water flow rate with various CNT-Ag loading amounts. The curves represent the variations of the CNT-Ag layer thickness and pure water flow rate as a function of the CNT-Ag loading onto the CNT-Ag nanofilter. The water flow rate experiments were carried out at room temperature. This experiment was repeated in each condition by three times. CNT: carbon nanotube.

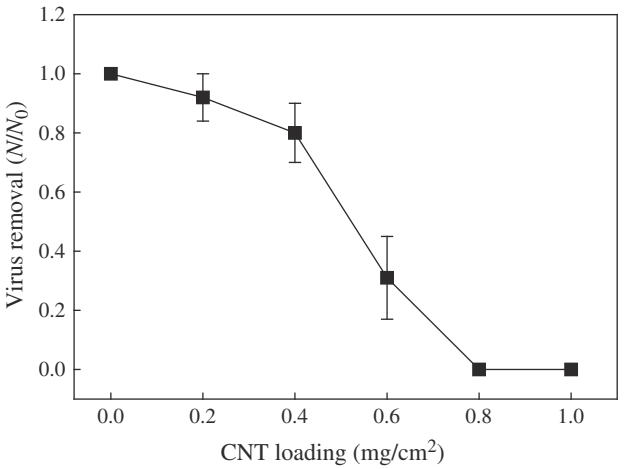

Fig. 8 – Virus removal by the CNT-Ag nanofilter at various CNT-Ag loadings. Initial virus concentration (N$_0$) was 1.1 × 10^4 copies/mL. Viral passage (N) was normalized by the initial concentration for the corresponding run (N$_0$). The graph describes the normalized residual virus concentration at the filter outlet (N/N$_0$) *versus* the CNT-Ag layer thickness. The experiments were carried out at a pressure of 5 kgf/cm^2 at room temperature. The experiments were repeated four times and showed reproducible results. CNT: carbon nanotube.

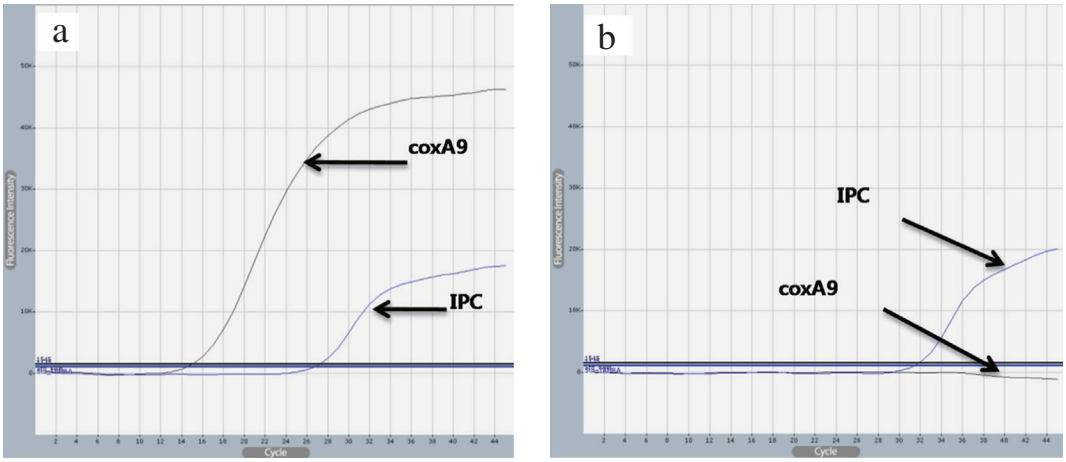

Fig. 9 – Removal of coxA9virus at 0.8 mg/cm^2 CNT-Ag loadings. The result of the real-time qPCR analysis (a) in the absence (control) and (b) in the presence of the CNT-Ag nanofilter. CNT: carbon nanotube.

removed in the control filter because the pore size was larger than the virus. However, no signal of coxA9 virus was detected in the 0.8 mg/cm^2-CNT-Ag nanofilter. This result clearly showed that coxA9 viruses were removed from the water. To demonstrate this phenomenon, the pore size of the 0.8 mg/cm^2-CNT-Ag filter was determined by capillary flow analysis. Fig. 10 shows the pore size distribution of the CNT-Ag nanofilter layer surface. The pore size of the CNT-Ag filter varied from 0.035 to 0.047 μm at a CNT-Ag load of 0.8 mg/cm^2. The average pore diameter at the surface of the CNT-Ag nanofilter is 38 nm. Although the size of a few pores was distributed below 50 nm, the measured pore size of the CNT-Ag nanofilter was higher than the size of the viruses (27–35 nm). The large pore size measured for the CNT-Ag filter is due to the method used for measuring the pore size distribution, in which the pore size distribution is assessed by measuring the size of air bubbles passing through the module. Therefore, errors in the measured size may be due to the expansion of the air bubbles. Thus, the actual pore size of the CNT-Ag nanofilter was assumed less than 38 nm.

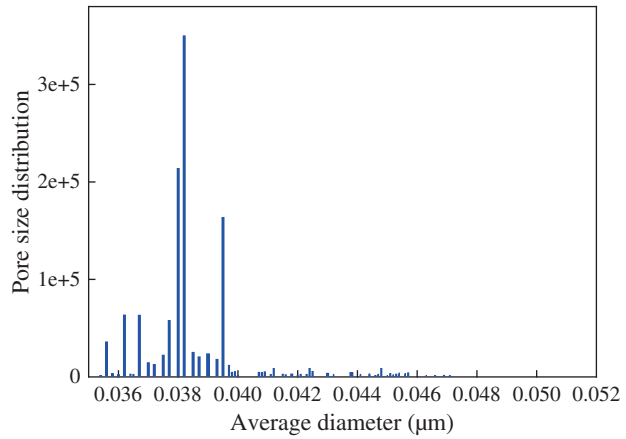

Fig. 10 – Pore size distribution of the 0.8 mg/cm^2 CNT-Ag-coated filter. CNT: carbon nanotube.

CNT-Ag nanofilters can also filter a mixture of two viruses. Fig. 11 shows the results of the real-time RT-qPCR analysis of two kinds of viruses (*i.e.*, Poliovirus and Norovirus). Poliovirus is composed of an RNA genome and a protein capsid. The viral particle is about 30 nm in diameter and has icosahedral symmetry (Foriers et al., 1990). Norovirus is a single-stranded RNA virus that can range in size from 27 to 35 nm (Wobus et al., 2006). The result of the filtration test showed that only the signals of the internal positive control (IPC), and not those of the Poliovirus and Norovirus, were amplified. Accordingly, the filtration experiment conducted on the mixed solution of Poliovirus and Norovirus confirmed that the viruses did not

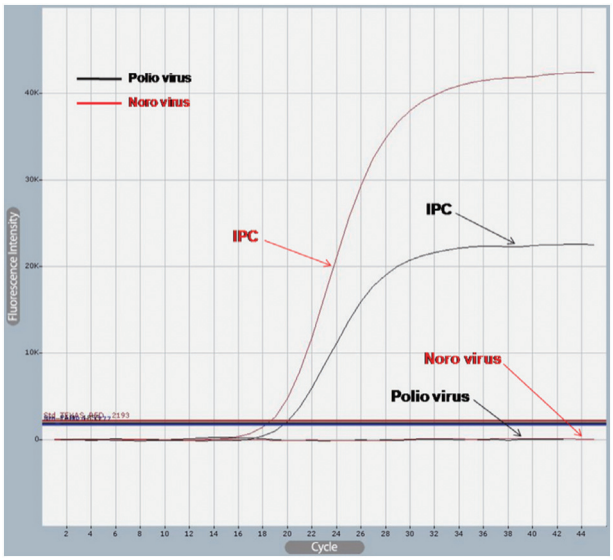

Fig. 11 – The results of the removal test of a mixture solution containing Poliovirus and Norovirus. Mixture solution was filtered through a CNT-Ag nanofilter and its content was subsequently analyzed using real-time RT-qPCR. CNT: carbon nanotube; RT-qPCR: Real-time reverse-transcription quantitative polymerase chain reaction.

pass through the CNT-Ag nanofilter. These results support the conclusion that viruses are removed from the water inside the CNT-Ag network layer by attaching to the fibrous CNT-Ag.

2.5. Bacterial removal and antibacterial activity of the CNT-Ag nanofilter

The use of the CNT-Ag nanofilters was also evaluated for the successful removal of bacterial contamination from drinking water. The gram-positive *S. aureus* and gram-negative *E. coli* have been widely used in bacteria-based experiments. *S. aureus* and *E. coli* live on the body surface of mammals and, sometimes, they cause infections. Furthermore, since these bacteria show the unique cell envelope structures of gram-positive and gram-negative bacteria, these strains were selected for our antibacterial activity test.

First, *S. aureus*, which is spherical in shape and 1000 nm in diameter, smaller than *E. coli*, was cultured at 37°C for 12 hr in a BHI liquid medium to test the bacterial removal ability of CNT-Ag. The cultured liquid medium was filtered through the CNT-Ag nanofilter, and the filtrate was smeared on the BHI plate medium and cultured at 37°C for 12 hr. The resulting photograph is shown in Fig. 12a. The growth of the bacterial colonies indicated that the liquid medium was not filtered through the nanoporous membrane, while lack of growth of the bacterial colonies suggested that the liquid medium was filtered through the nanoporous membrane. The results showed that when the *S. aureus* filtrate was smeared on the BHI plate medium, no colonies were formed on the plate (Fig. 12a), which indicated that *S. aureus* was effectively filtered out by the carbon nanotube-silver composite nanoporous membrane. This result shows that our CNT-Ag filter, which has nanosized-pores, can effectively remove microsized-bacteria from water.

Furthermore, our CNT-Ag filter has an antibacterial effect due to the Ag nanoparticles on the CNT surface. To test the antibacterial activity of the CNT-Ag nanofilter, 100 μL of *S. aureus* and *E. coli* culture media (103 CFU/mL) was smeared on a BHI plate medium on which a CNT-Ag nanofilter was placed as shown in Fig. 12b, c, and the cells were cultured at 37°C for 24 hr. Fig. 12b, c show that no colony was formed on the plates on which the CNT-Ag nanofilter was placed, which indicated that the CNT-Ag nanofilter had an antibacterial effect. This test showed that Ag nanoparticles have potent antibacterial activity against *S. aureus* and *E. coli* cells. The antibacterial activity of Ag nanoparticles is related to the formation of reactive oxygen species (ROS). The ROS generated by the Ag nanoparticles, such as superoxide anion (O_2^-), hydroxyl radical ($OH^\cdot$) and singlet oxygen ($^1O_2$), can not only cause damage to the cell membrane, but can also cause damage to the proteins, DNA, and intracellular systems such as the respiratory system (Kim et al., 2011). Moreover, the useful lifetime of a CNT-Ag composite nanoporous filter can be increased by manufacturing it according to the present method due to the antibacterial effect of the CNT-Ag nanofilter, which prevents biofouling (Gunawan et al., 2011).

3. Conclusions

In this study, our CNT-Ag nanofilter was specifically designed for the high-efficiency removal of various viruses and bacteria from water. First, the pore size of the filter was controlled according to the CNT-Ag composite loading amount. This allowed for a very small pore size (below 30 nm), which is suitable for filtration schemes such as nanosized virus and microsized bacteria removal. Second, the permeability of the CNT-Ag filter was improved by a plasma treatment process. After plasma treatment, the CNT-Ag filter was changed from having a hydrophobic surface to a very stable hydrophilic surface. Finally, the introduction of Ag nanoparticles on the CNT filter surface provided the nanofilter antibacterial activity and prevented biofouling. Moreover, the fact that additional processes to remove viruses and bacteria are not necessary provides a significant advantage in terms of manufacturing costs. Because of the small amount of CNT-Ag per filter area, as well as the ease of preparation through simple CNT-Ag dispersion and deposition on a base membrane, the production costs should not be very high. By considering all the advantages mentioned above, we believe that our CNT-Ag nanofilter provides satisfactory solutions for water treatment and other separation processes.

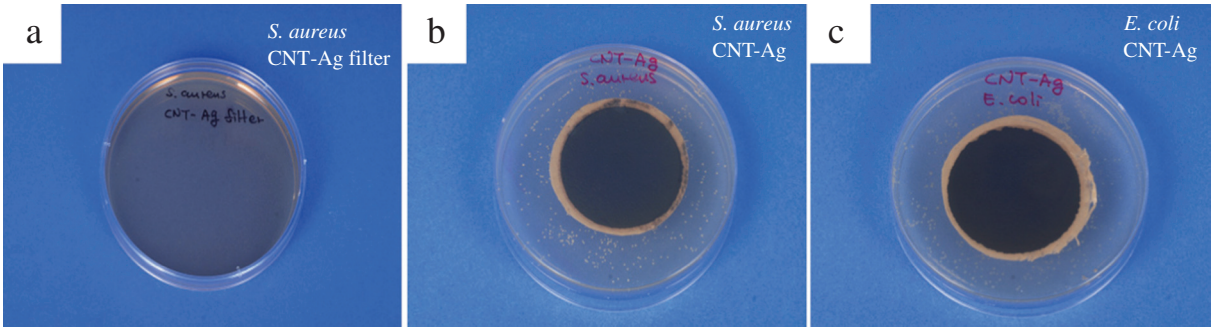

Fig. 12 – Removal of bacteria by using a carbon nanotube filter coated with Ag nanoparticles. (a) The absence of *S. aureus* colonies on the agar plate after filtration. The unfiltered water containing *S. aureus* (b) and *E. coli* (c) was cultured on an agar plate in the presence of the CNT-Ag nanofilter. In both cases, bacterial colonies grew on the agar and did not grow on the CNT-Ag nanofilter. CNT: carbon nanotube.

REFERENCES

Akhavan, O., Abdolahad, M., Abdi, Y., Mohajerzadeh, S., 2011. Silver nanoparticles within vertically aligned multi-wall carbon nanotubes with open tips for antibacterial purposes. J. Mater. Chem. 21 (2), 387–393.

Ayyappan, S., Subbanna, G.N., Srinivasa Gopalan, R., Rao, C.N.R., 1996. Nanoparticles of nickel and silver produced by the poyol reduction of the metal salts intercalated in montmorillonite. Solid State Ionics 84 (3-4), 271–281.

Brady-Estévez, A.S., Kang, S., Elimelech, M.A., 2008. Singlewalled-carbon-nanotube filter for removal of viral and bacterial pathogens. Small 4 (4), 481–484.

Brady-Estévez, A.S., Schnoor, M.H., Vecitis, C.D., Saleh, N.B., Ehmelech, M., 2010a. A multiwalled carbon nanotube filter: improving viral removal at low pressure. Langmuir 26 (18), 14975–14982.

Brady-Estévez, A.S., Schnoor, M.H., Kang, S., Elimelech, M., 2010b. SWNT-MWNT hybrid filter attains high viral removal and bacterial inactivation. Langmuir 26 (24), 19153–19158.

Brady-Estévez, A.S., Nguyen, T.H., Gutierrez, L., Elimelech, M., 2010c. Impact of solution chemistry on viral removal by a single-walled carbon nanotube filter. Water Res. 44 (13), 3773–3780.

Cha, S.I., Kim, K.T., Arshad, S.N., Mo, C.B., Hong, S.H., 2005. Extraordinary strengthening effect of carbon nanotubes in metal-matrix nanocomposites processed by molecular-level mixing. Adv. Mater. 17 (11), 1377–1381.

Di, Z.C., Ding, J., Peng, X.J., Li, Y.H., Luan, Z.K., Liang, J., 2006. Chromium adsorption by aligned carbon nanotubes supported ceria nanoparticles. Chemosphere 62 (5), 861–865.

Diallo, M.S., Savage, N., 2005. Nanoparticles and water quality. J. Nanoparticle Res. 7 (4-5), 325–330.

Ducamp-Sanguesa, C., Herrera-Urbina, R., Figlarz, M., 1993. Fine palladium powders of uniform particle size and shape produced in ethylene glycol. Solid State Ionics 63–65, 25–30.

Foriers, A., Rombaut, B., Boeyé, A., 1990. Use of high-performance size-exclusion chromatography for the separation of poliovirus and subviral particles. J. Chromatogr. 498 (1), 105–111.

Gunawan, P., Guan, C., Song, X.H., Zhang, Q.Y., Leong, S.S.J., Tang, C.Y., et al., 2011. Hollow fiber membrane decorated with Ag/MWNTs: toward effective water disinfection and biofouling control. ACS Nano 5 (12), 10033–10040.

Hinotsu, T., Jeyadevan, B., Chinnasamy, C.N., Shinoda, K., Tohji, K., 2004. Size and structure control of magnetic nanoparticles by using a modified polyol process. J. Appl. Phys. 95 (11), 7477–7479.

Iijima, S., 1991. Helical microtubules of graphitic carbon. Nature 354 (6348), 56–58.

Kang, S., Herzberg, M., Rodrigues, D.F., Elimelech, M., 2008a. Antibacterial effects of carbon nanotubes: size does matter. Langmuir 24 (13), 6409–6413.

Kang, S., Mauter, M.S., Elimelech, M., 2008b. Physicochemical determinants of multiwalled carbon nanotube bacterial cytotoxicity. Environ. Sci. Technol. 42 (19), 7528–7534.

Kang, S., Mauter, M.S., Elimelech, M., 2009. Microbial cytotoxicity of carbon-based nanomaterials: implications for river water and wastewater effluent. Environ. Sci. Technol. 43 (7), 2648–2653.

Kim, K.T., Cha, S.I., Hong, S.H., 2007. Hardness and wear resistance of carbon nanotube reinforced Cu matrix composites. Mater. Sci. Eng. A 449–451, 46–50.

Kim, K.T., Eckert, J., Menzel, S.B., Gemming, T., Hong, S.H., 2008. Grain refinement assisted strengthening of carbon nanotube reinforced copper matrix composites. Appl. Phys. Lett. 92 (12), 121901–121903.

Kim, S.H., Lee, H.S., Ryu, D.S., Choi, S.J., Lee, D.S., 2011. Antibacterial activity of silver-nanoparticles against *Staphylococcus aureus* and *Escherichia coli*. Korean J. Microbiol. Biotechnol. 39 (1), 77–85.

Kim, A., Lim, S., Peck, D.H., Kim, S.K., Lee, B., Jung, D., 2012. Preparation and characteristics of SiOx coated carbon nanotubes with high surface area. Nanomaterials 2 (4), 206–216.

Li, Y.H., Ding, Z., Luan, K., Di, Z.C., Zhu, Y.F., Xu, C.L., et al., 2003. Competitive adsorption of Pb^{2+}, Cu^{2+} and Cd^{2+} ions from aqueous solutions by multiwalled carbon nanotubes. Carbon 41 (14), 2787–2792.

Liu, X.Y., Pan, D., Choi, H., Lee, J.K., 2013. Superamphiphilic Ag-CNTs electrode by atmosphere plasma treatment. Curr. Appl. Phys. 13, S122–S126.

Lu, C.S., Chung, Y.L., Chang, K.F., 2005. Adsorption of trihalomethanes from water with carbon nanotubes. Water Res. 39 (6), 1183–1189.

Melnick, J.L., Rhian, M., Warren, J., Breese, S.S., 1951. The size of Coxsackie viruses and Lansing poliomyelitis virus determined by sedimentation and ultrafiltration. J. Immunol. 67 (2), 151–162.

Park, H.S., Gong, M.S., 2012. Facile preparation of nanosilver-decorated MWNTs using silver carbamate complex and their polymer composites. Bull. Kor. Chem. Soc. 33 (2), 483–488.

Peng, X.J., Luan, Z.K., Ding, J., Di, Z.H., Li, Y.H., Tian, B.H., 2005. Ceria nanoparticles supported on carbon nanotubes for the removal of arsenate from water. Mater. Lett. 59 (4), 399–403.

Rahaman, M.S., Vecitis, C.D., Elimelech, M., 2012. Electrochemical carbon-nanotube filter performance toward virus removal and inactivation in the presence of natural organic matter. Environ. Sci. Technol. 46 (3), 1556–1564.

Schoen, D.T., Schoen, A.P., Hu, L.B., Kim, H.S., Heilshorn, S.C., Cui, Y., 2010. High speed water sterilization using one-dimensional nanostructures. Nano Lett. 10 (9), 3628–3632.

Upadhyayula, V.K.K., Deng, S., Mitchell, M.C., Smith, G.B., 2009. Application of carbon nanotube technology for removal of contaminants in drinking water: a review. Sci. Total Environ. 408 (1), 1–13.

Wang, Z.J., Kwon, D.J., Gu, G.Y., Lee, W.I., Park, J.K., DeVries, K.L., et al., 2013. Evaluation of interfacial properties of atmospheric pressure plasma-treated CNT-phenolic composites by dual matrix fragmentation and acoustic emission tests. Compos. Part A 52, 151–158.

Wobus, C.E., Thackray, L.B., Virgin, H.W., 2006. Murine norovirus: a model system to study norovirus biology and pathogenesis. J. Virol. 80 (11), 5104–5112.

Yan, H., Gong, A.J., He, H.S., Zhou, J., Wei, Y.X., Lü, L., 2006. Adsorption of microcystins by carbon nanotubes. Chemosphere 62 (1), 142–148.

Zhao, B., Zhang, L., Wang, X.Y., Yang, J.H., 2012. Surface functionalization of vertically-aligned carbon nanotube forests by radio-frequency Ar/O_2 plasma. Carbon 50 (8), 2710–2716.